

Comparing perturbation models for evaluating stability of neuroimaging pipelines

Gregory Kiar¹ , Pablo de Oliveira Castro², Pierre Rioux¹,
Eric Petit³, Shawn T Brown¹, Alan C Evans¹
and Tristan Glatard⁴

The International Journal of High
Performance Computing Applications
2020, Vol. 34(5) 491–501
© The Author(s) 2020



Article reuse guidelines:

sagepub.com/journals-permissions

DOI: 10.1177/1094342020926237

journals.sagepub.com/home/hpc



Abstract

With an increase in awareness regarding a troubling lack of reproducibility in analytical software tools, the degree of validity in scientific derivatives and their downstream results has become unclear. The nature of reproducibility issues may vary across domains, tools, data sets, and computational infrastructures, but numerical instabilities are thought to be a core contributor. In neuroimaging, unexpected deviations have been observed when varying operating systems, software implementations, or adding negligible quantities of noise. In the field of numerical analysis, these issues have recently been explored through Monte Carlo Arithmetic, a method involving the instrumentation of floating-point operations with probabilistic noise injections at a target precision. Exploring multiple simulations in this context allows the characterization of the result space for a given tool or operation. In this article, we compare various perturbation models to introduce instabilities within a typical neuroimaging pipeline, including (i) targeted noise, (ii) Monte Carlo Arithmetic, and (iii) operating system variation, to identify the significance and quality of their impact on the resulting derivatives. We demonstrate that even low-order models in neuroimaging such as the structural connectome estimation pipeline evaluated here are sensitive to numerical instabilities, suggesting that stability is a relevant axis upon which tools are compared, alongside more traditional criteria such as biological feasibility, computational efficiency, or, when possible, accuracy. Heterogeneity was observed across participants which clearly illustrates a strong interaction between the tool and data set being processed, requiring that the stability of a given tool be evaluated with respect to a given cohort. We identify use cases for each perturbation method tested, including quality assurance, pipeline error detection, and local sensitivity analysis, and make recommendations for the evaluation of stability in a practical and analytically focused setting. Identifying how these relationships and recommendations scale to higher order computational tools, distinct data sets, and their implication on biological feasibility remain exciting avenues for future work.

Keywords

Neuroimaging, diffusion MRI, stability, Monte Carlo Arithmetic

1. Introduction

A lack of computational reproducibility (Peng, 2011) has become increasingly apparent in the last several years, calling into question the validity of scientific findings affected by published tools. Reproducibility issues may have numerous sources of error, including undocumented system or parametrization differences and the underlying numerical stability of algorithms and implementations employed. While containerization can mitigate the extent of machine-introduced variability, understanding the effect that these sources of error have on the encapsulated numerical algorithms remains difficult to explore. In simple cases where algorithms are differentiable or invertible, it is possible to obtain closed-form solutions for their stability.

However, as software pipelines grow, containing multiple complex steps, using non-linear optimizations and non-differentiable functions, the stability of these algorithms must be explored empirically.

¹ Department of Biomedical Engineering, McGill University, Montreal, Canada

² Department of Computer Science, University of Versailles, Versailles, France

³ Exascale Computing Lab, Intel, Paris, France

⁴ Department of Computer Science, Concordia University, Montreal, Canada

Corresponding author:

Gregory Kiar, Department of Biomedical Engineering, McGill University, 3801 Rue University, Montreal, Quebec H3A 0G4, Canada.

Email: gregory.kiar@mail.mcgill.ca

As neuroscience has evolved into an increasingly computational field, it has suffered from the same questions of numerical reproducibility as many other domains (Baker, 2016). In particular, neuroimaging often attempts to fit alignments, segmentations, or models of the brain using few samples with variable signal-to-noise properties. The nature of these operations leaves them potentially vulnerable to instability when presented with minor perturbations in either the data themselves or their processing implementations. High performance computing (HPC), commonly used in neuroimaging, is one such perturbation. As data sets grow in size, the adoption of HPC environments becomes a necessity. Given that these environments are highly heterogeneous in terms of hardware, operating systems, and parallelization schemes, this heterogeneity has been shown to compound with tool-specific instabilities and impact results (Glatard et al., 2015).

The independent evaluation of atomic pipeline components may be feasible in some cases, as was done by Skare et al. (2000). Here, the authors computed the theoretical conditioning of various tensor models used in diffusion modeling and compared these values to the observed variances in tensor features when fit on simulated data. While approaches like the above provide valuable insights to algorithms and their implementations independently, the impact of these stepwise instabilities within composite pipelines remains unknown. Even if one were able to evaluate each step within a pipeline, identifying the impact these instabilities may have on a result when composed together, both structurally and analytically, remains practically difficult to evaluate.

Various forms of instability have been observed in structural and functional magnetic resonance (MR) imaging, including across operating system versions (Glatard et al., 2015), minor noise injections (Lewis et al., 2017), as well as data set or implementation of theoretically equivalent algorithms (Bowring et al., 2018; Klein et al., 2009). These approaches may have practical applications in decision-making, such as deciding which tool/implementation should be used for an experiment. However, they are relatively far removed from the underlying numerical instabilities being observed. Recent advances in numerical analysis allow for the replacement of floating-point operations with Monte Carlo Arithmetic simulations (Parker, 1997) which inject a random zero-bias rounding error to operations for a target floating-point precision (Frechtling and Leong, 2015; Parker, 1997). This method can be used for evaluating the numerical stability of tools by wrapping existing analyses (Frechtling and Leong, 2015) and providing a foothold for scientists wishing to explore the space of their pipeline's compound instabilities (Denis et al., 2016).

In this article, we explore the effect of various perturbations on a typical diffusion MR image processing pipeline through the use of (i) targeted noise injections, (ii) Monte Carlo Arithmetic, and (iii) varying operating systems to identify the quality and severity of their impact on derived data. This evaluation will inform future work exploring the

stability of these pipelines and downstream analyses dependent upon them. The processing pipeline selected for exploration is Dipy (Garyfallidis et al., 2014), a popular tool that generates structural connectivity maps (connectomes) for each participant. The pipeline accepts de-noised and co-registered images as inputs and then performs two key processing steps: tensor fitting and tractography. We demonstrate the relative impact that each of the tested perturbation methods has on the resulting connectomes and explore the nature of where these differences emerge.

2. Methods

All processing described below was run using servers provided by Compute Canada. Software pipelines were encapsulated and run using Singularity (Kurtzer et al., 2017) version 2.6.1. Tasks were submitted, monitored, and provenance captured using Clowdr (Kiar et al., 2019) version 0.1.2-1. All codes for performing the experiments and creating associated figures are available on GitHub at <https://github.com/gkiar/stability> and <https://github.com/gkiar/stability-mca>, respectively.

2.1. Data set and pre-processing

The data set used for processing is a 10-session subset of the Nathan Kline Institute Rockland Sample (NKI-RS) data set (Nooner et al., 2012). This data set contains high-fidelity structural, functional, and diffusion MR data and is openly available for research consumption. The 10 sessions used were chosen by randomly selecting 10 participants and selecting their alphabetically first session of data. These data were pre-processed prior to the modeling evaluated here using a standard de-noising and image alignment pipeline (Kiar, 2019) built upon the FSL toolbox (Jenkinson et al., 2012). The steps in this pipeline include eddy current correction, brain extraction, tissue segmentation, and image registration. The boundary between white and gray matter was obtained by computing the difference between a dilated version of the white matter mask and the original. Data volumes at this stage of processing are four-dimensional and variable in spatial extent (first three dimensions) with a fixed number of diffusion directions (fourth dimension), totaling approximately $100^3 \times 137$ voxels in each case.

2.2. Modeling

After pre-processing the raw diffusion data using FSL, structural connectomes were generated for an 83-region cortical and subcortical parcellation (Cammoun et al., 2012) using Dipy (Garyfallidis et al., 2014). A six-component tensor model was fit to the diffusion data residing within white matter. Seeds were generated in a $2 \times 2 \times 2$ arrangement for each voxel within the boundary mask, resulting in eight seeds per boundary voxel. Deterministic tracing was then performed using a half-voxel step size,

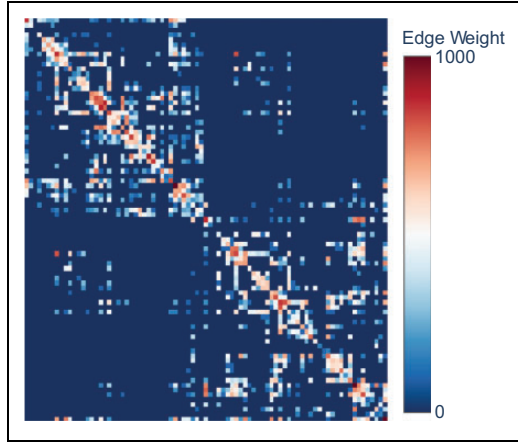


Figure 1. Example connectome. Each row and column corresponds to a region within the brain, and the intersection a connection between them. If no connection is found between regions, the edge strength is zero. If a streamline is found to connect two regions, the weight is incremented by 1. The resulting weights are the sum of all observed connections for every streamline traced within a brain image.

and streamlines shorter than three points in length were discarded as spurious. Once streamlines were generated, they were traced through the parcellation. Edges were added to the graph corresponding to the end points of each fiber and were weighted by the streamline count. This pipeline was implemented in Python, including a few components in Cython, and relies on the Numpy library for a large proportion of operations. Each resulting network is a square connectivity matrix of 83×83 edges, as shown in Figure 1. This pipeline was chosen as it is both common and simple relative to many alternatives.

2.3. Stability evaluation

Targeted and Monte Carlo perturbation modes were tested $100\times$ per image. Noise was represented by percent deviation of the Frobenius norm of a resulting connectome from the corresponding reference (no noise injection). A deviation of 50% indicates that the norm of the difference between the noisy and reference networks is 50% the size of the norm of the reference graph. This is formalized below in equation (1)

$$\%Dev(A, B) = \frac{\sqrt{\sum_{i=1}^m \sum_{j=1}^n |a_{ij} - b_{ij}|^2}}{\sqrt{\sum_{i=1}^m \sum_{j=1}^n |a_{ij}|^2}} \quad (1)$$

where A is the reference graph, B is the perturbed graph, and a_{ij} is an element therein at row i and column j .

The perturbation methods evaluated, presented below, are summarized in Table 1.

2.4. Subject-level variation

Comparison between subjects will be used as a reference error. If the differences observed by other methods are

Table 1. Description of perturbation modes.

Permutation	Description
X-subject	Pairwise comparison of sessions based on Subject ID.
1-voxel	Intensity value doubled for either single (one voxel in entire 4D volume) or independent (one voxel per 3D sub-volume) voxels.
MCA	Simulation of all floating-point operations in Python (Python and Cython-compiled libraries).
RR	Simulation of all rounding operations in Python or the Full Stack (BLAS and LAPACK, Python and Cython-compiled libraries).
X-OS	One of Ubuntu 16.04 or Alpine 3.7.1.

similar in magnitude to the subject-level difference, then the validity of the processed networks for use in downstream phenotypic analysis becomes questionable as subjects cannot be reliably distinguished from one another. This error is computed as the pairwise distance between all 10 subjects included in this cohort.

2.5. Targeted noise

The goal of targeted noise was to inject data perturbations sufficiently small that the resulting images would be indistinguishable from the original. This is meant to test the lower bound of noise sensitivity for processing pipelines. The type of targeted noise used here will be referred to as 1-voxel noise and is similar to the method employed by Lewis et al. (2017). In our case, the intensity of a single voxel in the defined range will be scaled based on a scaling factor. The voxels modified in this case were randomly generated within the mask of brain regions being modeled by the pipeline.

The two modes of 1-voxel noise injection tested here were: (a) a single voxel per entire image of size (X, Y, Z, D) (approximately $100^3 \times 137$ for all images), or (b) a single voxel per 3D volume of size (X, Y, Z) (approximately 100^3 for all images), and are referred to as “single” and “independent” modes, respectively. While the number of perturbed voxels in the independent case is approximately $100\times$ larger, the intensity of magnification was consistent as in both cases the original voxel intensities were doubled.

2.6. Monte Carlo Arithmetic

Verificarlo (Denis et al., 2016) is an extension of the LLVM compiler which automatically instruments floating-point operations at build-time for software written in C, C++, and Fortran. Once compiled with Verificarlo, the Monte Carlo emulation method and target precision can be set as environment variables. For all simulations, a rounding error on the least significant floating-point bit in the mantissa (bit 53) was introduced. The simulations were computed using the custom QUAD backend which is

optimized to reduce computation time over the traditional MCALIB MPFR backend leveraging GNU's multiple precision library (Frechtling and Leong, 2015). Noise through Verificarlo can be injected as "Precision Bounded," simulating floating-point cancellations, "Random Rounding (RR)," simulating only rounding errors on computation, and "MCA," which includes both of these modes. A particularity of the RR mode is that it only injects rounding noise on inexact floating-point operations (i.e. operations that have a rounding error in IEEE-754 at the target precision). Therefore, RR mode preserves the original exact operations, it is a more conservative noise simulation. We used both the RR and MCA modes of simulation.

Verificarlo was used to instrument tools in two modes we will refer to as "Python" and "Full Stack." In the Python instrumentation, the core Python libraries were recompiled with Verificarlo as well as any subsequently installed Cython libraries. In the Full Stack instrumentation, BLAS and LAPACK were also recompiled, meaning that Numpy, a dominant Python library for linear algebra, was also instrumented. The Full Stack implementation did not run successfully using the MCA mode. We suspect that some libraries require exact floating-point operations or are sensitive to cancellation errors, so only the RR mode was able to be evaluated for the Full Stack. These instrumentations took several working days (including substantial cumulative compilation times) for the authors to refine, and the images are available on DockerHub at [gkiar/fuzzy-python](https://github.com/gkiar/fuzzy-python).

2.7. Operating system variation

Operating system noise was evaluated across Alpine Linux 3.7.1 and Ubuntu 16.04. Alpine is a lightweight distribution which comes with minimal packages or libraries, and Ubuntu is a popular Linux distribution with a large user and development community. Alpine was chosen as its lightweight nature makes it an efficient choice for the packaging and distribution of libraries in containers for scientific computing, reducing the overhead of shipping code toward data sources. Ubuntu was chosen due to its high adoption and community support by major libraries. While Alpine comes with a minimal set of libraries, a core difference between these systems as noted by DistroWatch (<https://distrowatch.com/>) is their dependence on a different version of the Linux kernel. While numerical differences between operating systems are likely the result of compilers (Sawaya et al., 2017) and installed libraries, the purpose of testing across operating systems explicitly rather than combinations of specific tools is to recreate a real-world setting in which typical scientific users observe numerical differences across equivalent high-level pipelines.

Ubuntu was used as the base operating system for all simulations other than this comparison. The variability observed across operating systems was aggregated across participants and included as a reference margin of error.

2.8. Aggregation of simulated graphs

To structurally evaluate each simulation setting, connectomes were aggregated within setting and subject combinations. Several aggregation methods were explored to preserve various sensitivity and stability properties across the aggregated graphs. In each case, the operations are performed edge-wise, so the aggregated graph is not guaranteed to be single graph in the set of perturbed graphs. The aggregation operations are the edge-wise mean and the 0th (minimum), 10th, 50th (median), 90th, and 100th (maximum) percentiles. The mean aggregate will include a non-zero weight for every edge which appears in at least one simulation, and the 0th and 100th percentiles will include the lowest and highest observed weight for every edge, respectively. The 90th, 50th, and 10th percentiles increasingly aggressively filter edges based on their prominence across simulations. The combination of percentile aggregates also enables isolation of the most spurious edges, such as by taking the difference of maximum and minimum aggregates. A volatile aggregate was created to this effect which consists of edges which are found in the maximum aggregate but not the minimum aggregate. Note that in this case, the weight for these edges is not implied and can be defined as an alternative function of the graph collection, such as mean, but as the weight does not appear when comparing binary edges, no recommendation for this weighting is made here.

3. Results

All perturbation modes were applied to either the input data or post-processing pipeline described in Section 2.2 and were evaluated according to equation (1).

3.1. Perturbation-induced differences

Figure 2 shows the percentage deviation for each simulation mode on 10 subjects. Introduced perturbations show highly variable changes in resulting connectomes across both the perturbation model and subject, ranging from no change to deviations equivalent to difference typically observed across subjects. For the 10 subjects tested, we see that the Python-instrumented MCA and RR pipelines resulted in the largest deviation from the reference connectome. In these cases, we also see that the results are modal, where each subject has discrete states that may be settled in, some of which result in deviations comparable to subject-level noise. This modality is likely due to minor differences introduced at crucial branch points which then cascaded throughout the pipeline. This hypothesis is supported by observing that the Full Stack implementation with RR perturbations shows a continuous distribution of differences that are highly variable in intensity, ranging from no deviation to subject-level in some cases for some subjects, which are explored in Section 3.2.

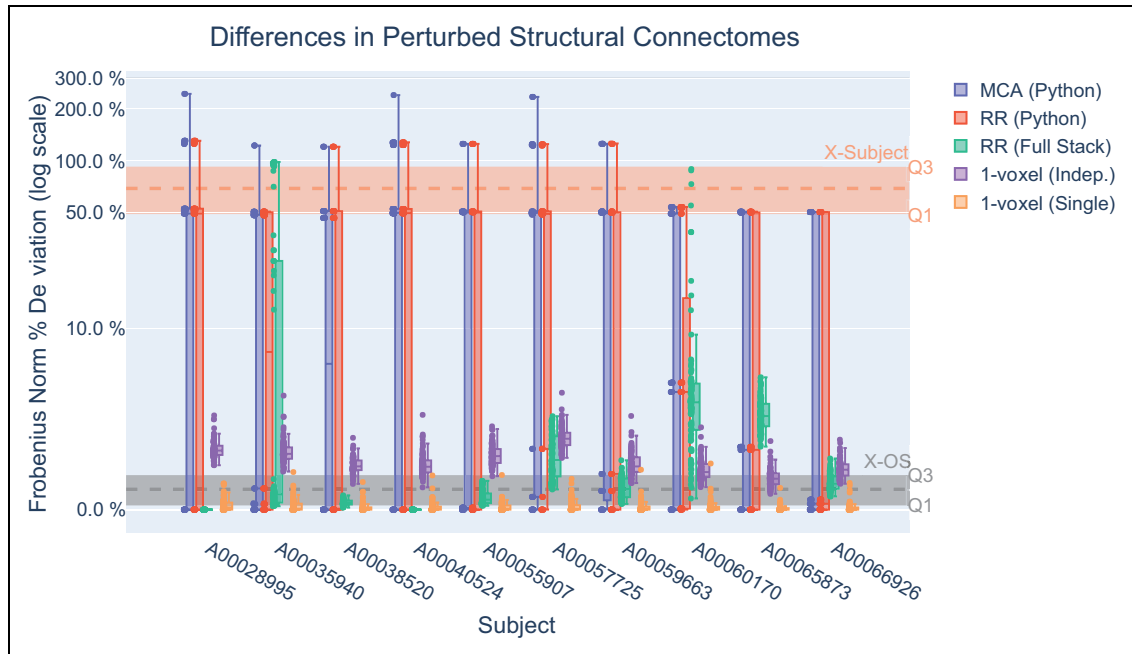


Figure 2. Comparison of perturbation modes. As evaluated by the percent deviation from reference in the Frobenius norm of a resulting connectome, each of the 10 processed subjects were reprocessed $100\times$ for each perturbation method. We see that the MCA and RR (Python) methods resulted in distinct modes for the outputs in all cases reaching extreme deviations equivalent to cross-subject variation. The RR (Full Stack) method shows high variability across subjects, and only reaching cross-subject variation in the case of two subjects. The 1-voxel methods result in considerably less deviation from reference and are more consistent across subjects than the RR (Full Stack) method.

The 1-voxel independent mode unsurprisingly produces larger changes than the 1-voxel single mode. These changes are larger than or comparable to operating system variability, respectively, resulting in small deviations from the reference, and are relatively minor in comparison to the extremes observed with Monte Carlo Arithmetic. Operating system deviations are very low or even zero in some cases. In all perturbation settings, we can see that there is large variability both across simulations on the same data and across subjects.

3.2. Progression of deviations in a continuous setting

In the case of subject A00035940, the Full Stack RR perturbations led to a continuous distribution of outputs, ranging in difference from none to subject-level from the reference. Figure 3 explores the progression of these deviations by visualizing the difference connectome for samples along various points of this distribution. In the center, we show the reference connectome, and surrounding it the difference graph for a simulated sample labeled %Dev from this reference. In this case, we can see a progression of structurally consistent deviations. In particular, edges corresponding to regions in the left hemisphere become increasingly distorted (bottom-right portion of the connectome), whereas the within-hemisphere connectivity for the right hemisphere (top-left portion) remains largely intact in all cases except the extreme difference case. We notice in all cases that the

connectivity between regions is decreasing until the edges disappear entirely. While this behavior is not consistent across all subjects, this observation suggests a peculiarity in the quality of data in this region for the subject in question. This could be due to artifacts caused by motion or other factors, ultimately reducing the stability of modeling connectivity in this region.

3.3. Structural properties of introduced perturbation

While the case investigated above notably showed a significant degradation of regional signal quality for Full Stack RR noise in a single subject, Figure 4 explores the relative change in connectivity from the reference for each perturbation mode and subject. Edges in the presented graphs are weighted by their standard deviation across all simulations for that participant and colored as positive or negative deviations based on whether the mean weight for all simulations was greater or lower than the reference weight, respectively. All edges with a standard deviation of 0 across all simulations were greened out for clarity.

For the Python-instrumented MCA and RR implementations, edge weight was generally inflated nonspecifically for existing edges in the reference connectome for all subjects. The Full Stack RR implementation shows significant variability across subjects, where the number of affected edges ranges from none to all. In each case where there exists some deviation, intensities appear to be spatially linked, suggesting the differences may be due to variable

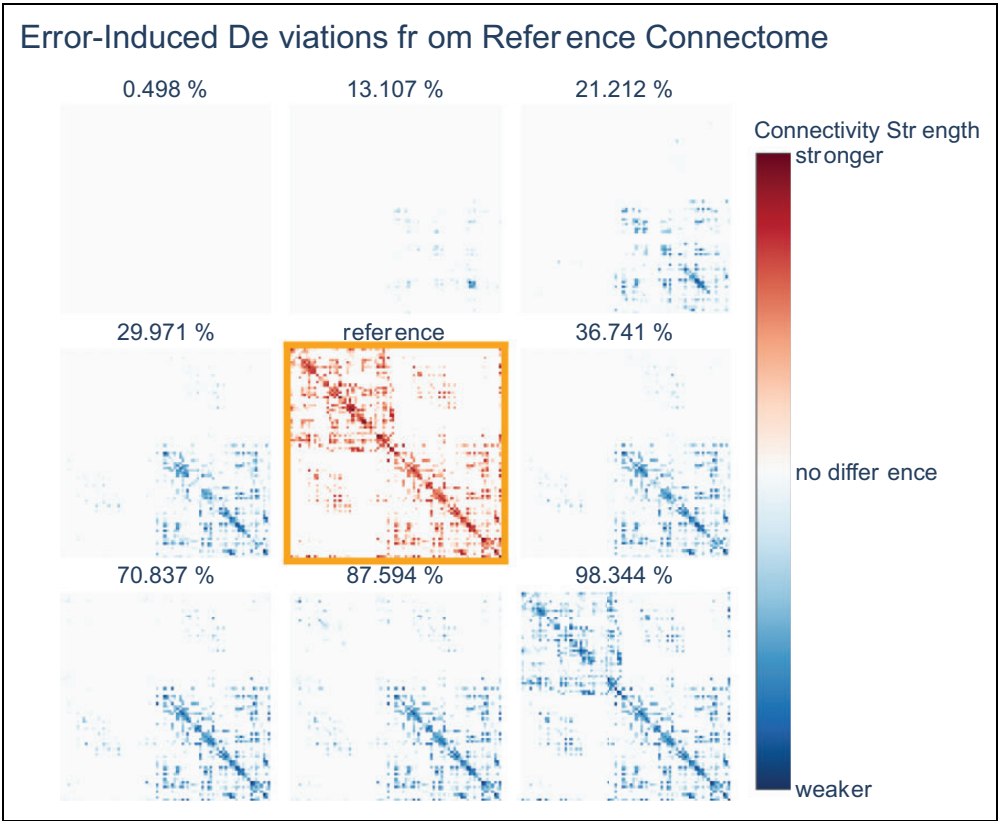


Figure 3. Structure of deviations. Shown in increasing deviation from left–right and top–bottom, with the reference in the center, are the difference connectomes observed for the RR (Full Stack) perturbations of subject A00035940. In this case, the left hemisphere (bottom-right portion of the graph) begins to degrade quickly, eventually reaching an almost complete loss in signal.

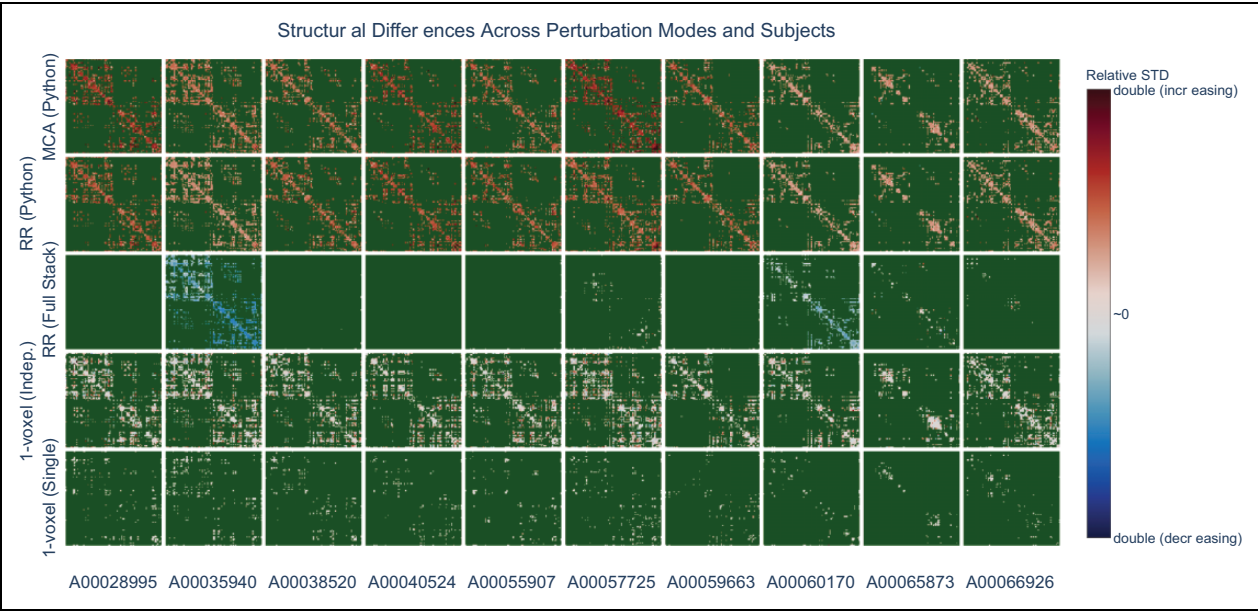


Figure 4. Perturbation introduced structural differences. The variance of each edge is shown relative to the reference edge strength, and colored either red or blue based on the mean perturbed weight was higher or lower than that of the reference, respectively. Edges which experienced no variation were colored as green to be distinct from all edges which experience any variation.

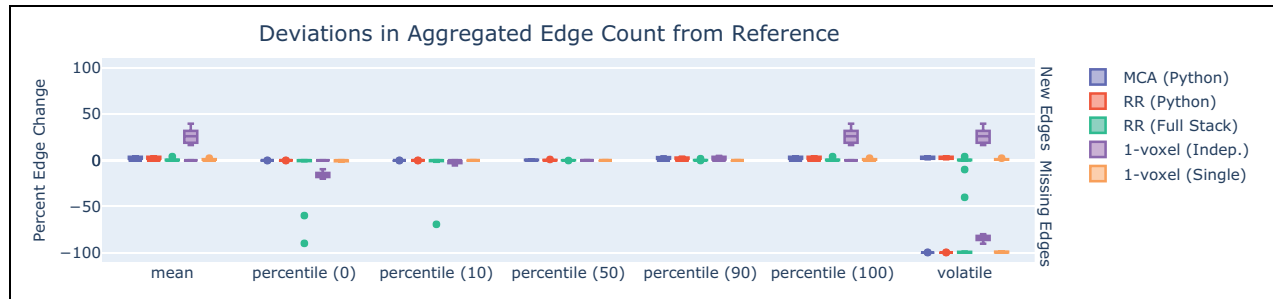


Figure 5. Gain and loss of edges in aggregation of simulations. The relative gain and loss of edges is shown for each aggregation method and perturbation method in terms of binary edge count. The volatile aggregation is the difference between 100th percentile aggregates, and it contains all edges which do not appear in every graph. The volatile set of edges for each of MCA (Python), RR (Python), RR (Full Stack), 1-voxel (independent), and 1-voxel (single) contain 2.5%, 2.5%, 18.5%, 43.0%, and 1.7% of the number of edges found in the reference, respectively. In the worst case, 1-voxel (independent), this means that the existence of nearly half the edges in the graph fail to have consensus across the simulations. RR: Random Rounding.

quality in the underlying data. In this case, Monte Carlo Arithmetic may have served to shed light on poor signal-to-noise properties present within regions of the images being modeled.

For 1-voxel noise, the differences introduced across independent injections impacted a larger portion of edges than single injections, unsurprisingly. By design (i.e. injection at random locations for each simulation), the deviations appear nonspecifically spatially distributed. However, 1-voxel noise could be modified to spatially constrain the location for noise injection regionally, allowing the evaluation of modeling for particular substructures within the images.

3.4. Aggregation across simulations

For each simulation method there existed a graph nearly identical to the reference, but the variability introduced by these simulations were highly variable both in terms of the method of perturbation used and the data set being processed. The aggregation of the simulated graphs into a consensus graph allows features of this variation to be encoded implicitly in connectomes which may be used for downstream analyses. Figure 5 shows the relative percentage of added and missing edges for each setting across all subjects using a variety of such aggregation methods.

By aggregating the simulated connectomes in a variety of methods, the resulting edges would be a product of applying some filter to the set of observed edges and succinctly represented in a single graph. While minor deviations in one edge may reduce the strength of connectivity between two strongly linked regions, the addition of a connection between two regions which were previously unconnected may be significant in one aggregation method but ignored in another. In the case of the above example, despite the strength of connectivity remaining low between the newly connected nodes many graph theoretic measures rely on binarized graphs and may be considerably affected, such as the degree.

We notice that the 1-voxel independent (i.e. single voxel per 3D volume) method shows the most variability across

each aggregation method. Where all of the MCA-derived methods perturb the pipeline nonlocally, both epsilon-level methods add local noise at arbitrary locations. This distinction seems to manifest in more widely added or knocked-out edges for the 1-voxel cases, as the location of noise may have considerable impact on a multitude of nearby fibers, where MCA methods have a zero-bias noise globally, meaning all deviations from the reference are spurious and due to numerical error rather than the introduction of a systemic change that sheds light on an underlying cascading instability.

Unsurprisingly, the only aggregation method which shows considerable amount of both new and missing edges is the volatile technique, which takes edges that exist in the binary difference of 100th and 0th percentile graphs, eliminating all extremely stable edges from the graph (i.e. those which exist for the reference and all simulations). While the mean sparsity of the reference graphs is 0.30, meaning 30% of possible connections have nonzero weight on average, the sparsity of the volatile aggregates ranges from 0.005 to 0.130, or the aggregates contain between 2.5% and 43.0% the number of edges as the reference graphs.

3.5. Comparison of simulation performance

While the application of each perturbation model tested sheds light on different properties of pipeline stability, the resource consumption of these methods has significant bearing when processing data in the context of a real experiment often consisting of dozens to hundreds of subjects worth of data. In this experiment, a single unperturbed pipeline execution took approximately 20 min using one core and 6 GB of RAM. Figure 6 shows the relative time on CPU for a single simulation of each method tested, relative to the reference task with no instrumentation. For Monte Carlo Arithmetic-instrumented executions, we expect to see a considerable increase in computation time as additional overhead is added to each floating-point operation. In the case of 1-voxel noise, it is expected to see a minor increase in computation time as the perturbed data volumes

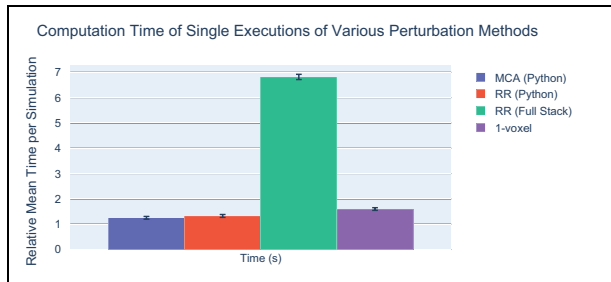


Figure 6. Computation time for each perturbation method. Shown in relative time to the reference execution, plotted is the average execution time for the perturbation methods. MCA and RR (Python) have a small increase in computation time per run, as few floating-point operations were instrumented in these settings. The RR (Full Stack) method has nearly a $7\times$ slowdown. In this case, all floating-point operations were instrumented, but the slowdown of less than the estimated $100\times$ would suggest that the bulk of computation time is not spent on floating-point arithmetic. The 1-voxel implementations had a minor slowdown due to the regeneration of data prior to pipeline execution. In every case, the real-world slowdown is $S\times$ larger, where S is the number of simulations, in this case 100.

were generated at runtime, reducing the data redundancy on disk.

The Python MCA and RR modes show a slight increase in computation time to the reference task, whereas the Full Stack version approaches a nearly $7\times$ slowdown, on average. This discrepancy further supports the hypothesis stated above that floating-point logic implemented directly in Python, without the use of Numpy or external libraries, accounts for a minor portion of the total floating-point operations. As Verificarlo has been shown to increase the runtime of floating-point operations by approximately $100\times$ (Denis et al., 2016), this result suggests that the pipeline evaluated here is largely I/O limited. In the case of 1-voxel perturbations, we see a slowdown approximately equivalent to that of the Python instrumentation, not exceeding a $2\times$ increase. Across all executions, approximately 2000 CPU hours were consumed. While this is a small workload in the context of HPC, the required resources quickly reach the order of CPU years after extrapolating to the entire NKI-RS data set or others in neuroimaging.

4. Discussion

We have demonstrated through the application of multiple perturbation methods how noise can be effectively injected into neuroimaging pipelines enabling the exploration and evaluation of the stability of resulting derivatives. These methods operate by either perturbing the data sets or tools used in processing, resulting in a range of structurally distinct noise profiles and distributions which may each provide value when exploring the stability of analyses. While 1-voxel noise is injected directly into the data sets prior to analysis, MCA and RR methods iteratively add significantly smaller amounts of noise to each operation performed.

In the case of partial (Python) instrumentation with MCA and RR, distinct and considerably distinct modes emerged in all tested subjects. We hypothesize that software branching likely played a role leading to this unexpected result. As the majority of numerical analysis in Python is traditionally performed using the Numpy library, and therefore BLAS and LAPACK, it is possible that the error introduced by Python was allowed to cascade throughout the pipeline without correction, until the next Python branch point occurred and this repeated, eventually growing to the often subject-level differences observed. These modes would then be the result of a small number of instrumented numerically sensitive operations, leading to a bounded set of possible outcomes of an otherwise deterministic process. It is possible that these distinct modes could serve as upper bounds for the deviation due to instabilities within a pipeline, and this is an area for further exploration. Future work will also more closely instrument libraries with functionality that will enable the identification of crucial branch points, as this functionality is already present within Verificarlo. The identified crucial branch points could be leveraged for the reengineering of pipelines with more stable behavior and potentially shed light on new best practices.

An exciting application of MCA and RR (Python) analyses in cases where pipeline modification is not feasible is the generation of synthetic data sets. Using each mode or an aggregated collection of modes as samples in the MCA-boosted data set could potentially increase the statistical power of analyses for data sets which may suffer from small samples, or be used to increase the robustness of derivatives by bagging the results using an appropriate averaging technique for the simulated derivatives.

While the Python instrumentation with MCA and RR resulted in derivative modes, the Full Stack instrumentation with RR produced a continuous distribution of derivatives which were often less distinct from the reference results. Extending the hypothesis posited above, this continuous set of results may be due to a law of large numbers effect emerging when performing a considerable number of small perturbations, leading to a normalized error distribution and effectively a self-correction of deviations. Future work will test this hypothesis and consider the relationship between the fraction of instrumented floating-point operations and modality, as well as through the incremental profiling and evaluation of tools for the comparison of intermediate derivatives and their deviation from a reference execution. These experiments have the potential to provide more insight into the origin of instabilities in scientific pipelines and identify rich optimization targets.

As the significance of RR (Full Stack) perturbation was highly variable across participants, this technique could also be used for automated quality control, flagging high-variance subjects for further inspection or exclusion from analyses. From the top level, inspecting the regional degradation of signal across these perturbations as shown in Figure 3, researchers could lead a targeted interrogation

of their raw data sets to identify underlying causes of signal loss. Conversely, investigating which low-level BLAS operations contribute to the observed instabilities will allow researchers to clarify the link between ill-conditioning and so-called bad data directly within their pipelines. Upon characterizing this relationship it would be valuable to identify the point (if any) at which targeted N -voxel perturbations become equivalent to MCA-induced variability.

The differences observed when performing 1-voxel perturbations were often comparable in magnitude to the variation introduced across Operating Systems. As OS noise is not controlled and may differ greatly among distributions, package updates, and so on, it is likely an insufficiently descriptive evaluation method and should be used as a reference alongside others. The level of control made available through 1-voxel perturbations in terms of both locality and strength of noise makes it a flexible option that could potentially be used to target known areas of key importance for subsequent analyses. Due to the fact that these perturbations introduce a minor change to input images, this method could also be used for estimating global pipeline stability in a classical sense (i.e. conditioning).

While each of the perturbation modes showed distinct differences with respect to the magnitude and continuity of their induced deviations, Figure 4 illustrates that the structure of these deviations was also highly variable across both perturbation method and data. This suggests different applications and use cases for each perturbation method. While MCA and RR Python implementations impact connectomes globally, these could be applied to generate synthetic data sets. Full Stack RR is highly variable with respect to data set, suggesting possible applications in quality control, granted further work is performed to more fully understand the effect observed between this and the Python-only case. Both 1-voxel methods add noise locally and can test the sensitivity of specific pipeline components or regions of interest to variation. Other methods, such as automatic differentiation, could also be explored as possible avenues leading toward an understanding of the end-to-end conditioning of pipelines.

In addition to generating unstable derivatives which could be looked at or analyzed independently, this type of perturbation analysis enables the aggregation of derivatives. As is summarized in Figure 5, the method by which graphs or edges are aggregated can drastically change the construction of resulting graphs. While the mean and maximum (i.e. 100th percentile) methods both retain all edges that have appeared in even a single graph, the minimum (0th percentile) and other low-percentile aggregations require a stricter consensus of edges for inclusion in the final graph. A benefit of performing multiple aggregations is the composition of graphs with complex edge composition, such as the most volatile edges, as is shown in the final column of Figure 5. While the binary edge count in the

composite graphs varies in each of these methods, it is unclear how derived graph statistics will be affected, and that remains an exciting question for further exploration.

From a resource perspective, each of the perturbation methods evaluated requires multiple iterations to get a sense of the pipeline stability or build aggregates, here taken as 100 iterations. Though the MCA-based methods have the obvious disadvantage of extra computational overhead within each execution cycle of the pipeline, the noise-injection methods do not increase the computation time for a single pipeline execution itself but in this case added computational burden for the generation of synthetic data dynamically, reducing the redundancy of stored images on disk. While Verificarlo has been demonstrated to account for an approximately $100\times$ slowdown in floating-point operations (Denis et al., 2016), the largest slowdown observed in this pipeline is approximately a factor of 7, as shown in Figure 6. This suggests that the bulk of time on CPU for this pipeline is not spent on floating-point operations but perhaps other operations such as looping, data access, or manipulation of information belonging to other data types. While this slowdown is observed for the Full Stack implementation, the Python-only implementation is negligibly slower than the reference execution, suggesting that even fewer of the floating-point logic is directly written in Python. The slowdown in the 1-voxel setting is of a similar scale to that of the Python-only implementation, with the slowdown likely caused by the addition of two read and one write operations to the pipeline's execution (reading of simulation parameters and original image, application of simulation, and subsequent writing of perturbed image to temporary storage). Note that the figures shown in Figure 6 are for a single simulation, and real relative CPU time in each case would be $100\times$ larger for the experimental application of these methods.

The work presented here demonstrates that even low-order computational models such as a six-component tensor used in diffusion modeling are susceptible to noise. This suggests that stability is a relevant axis upon which tools should be compared, developed, or improved, alongside more commonly considered axes such as accuracy/biological feasibility or performance. The heterogeneity observed across participants clearly illustrates that stability is a property of not just the data or tools independently but their interaction. Characterization of stability should therefore be evaluated for specific analyses and performed on a representative set of subjects for consideration in subsequent statistical testing. Additionally, identifying how this relationship scales to higher order models is an exciting next step which will be explored. Finally, the joint application of perturbation methods with more complex post-processing bagging or signal normalization techniques may lead to the development of more numerically stable analyses while maintaining sensitivity that would be lost in traditional approaches such as smoothing.

5. Conclusion

All pipeline perturbation methods showed unique nonzero output noise patterns in low-order diffusion modeling, demonstrating their viability for exploring numerical stability of pipelines in neuroimaging. MCA and RR (Python)-instrumented pipelines resulted in a wide range of variability, sometimes equivalent to subject-level differences, and are recommended as possible methods to estimate the lower bound of stability of analyses, generation of synthetic data sets, and possible identification of Python-introduced critical branch points. RR (Full Stack) perturbations resulted in continuously distributed connectomes that were highly variable across data sets, ranging from negligible deviations to complete regional signal degradation. We provisionally recommend the use of RR (Full Stack) noise for automated quality control and identifying global pipeline stability. While 1-voxel methods result in considerably smaller maximum deviations than the MCA-based methods, they are far more flexible and enable evaluating the sensitivity of pipelines to minor local data perturbations. While the MCA-based methods are more computationally expensive than direct 1-voxel noise injections, the slowdown was found to be less significant in practice than the $100\times$ scaling factor estimated per floating-point operation, presumably due to a significant portion of the pipeline computation time being spent on data management or string and integer processing rather than the constant use of floating-point arithmetic.

In all cases, while tool instrumentation enables the parallelized simulation of a particular set of instructions, the aggregation of the simulated graphs is an essential component of the downstream analyses both when exploring the nature of instabilities or developing inferences upon the pipeline's derivatives. We recommend a percentile approach to aggregation, where the threshold can be adjusted based on the desired robustness of the resulting graphs. An advantage of percentile approaches is also that composite aggregates can be formed, isolating edges based on their prevalence across simulations. Further exploration of the distribution of perturbed results should be performed to conclude on the relevance of the aggregation used, as the desired aggregate should be close to the expected value of the distribution.

While both MCA and random-injection simulations are computationally expensive in that they require the evaluation of many simulations, they provide an opportunity to characterize processing modes that may emerge when analyzing either noisy data sets or unstable tools. This work also highlighted an important relationship between the noise properties of an incoming data set and the tool, validating the need to jointly evaluate the stability of tool–data set combinations.

Where this work demonstrates a range of numerical variation across minor changes in the quality of data or computation, it does not address the analytic impact of these deviations on downstream statistical approaches. This open

question, as well as the relative impact of normalization techniques on this process, presents avenues for research which will more clearly place these results in a biologically relevant context, allowing characterization of the functional impact of the observed instabilities.

Authors' note

This research was enabled in part by support provided by Calcul Quebec (<http://www.calculquebec.ca>) and Compute Canada (<http://www.computeCanada.ca>).

Acknowledgements

The authors would like to thank Dell and Intel for their collaboration and contribution of computing infrastructure. The authors would also like to thank their reviewers for thoughtful and insightful comments and suggestions.


Declaration of conflicting interests

The author(s) declared no potential conflicts of interest with respect to the research, authorship, and/or publication of this article.

Funding

The author(s) disclosed receipt of the following financial support for the research, authorship, and/or publication of this article: This research was financially supported by the Natural Sciences and Engineering Research Council of Canada (NSERC) (award no. CGSD3-519497-2018).

ORCID iD

Gregory Kiar  <https://orcid.org/0000-0001-8915-496X>

References

- Baker M (2016) 1,500 scientists lift the lid on reproducibility. *Nature* 533(7604): 452–454.
- Bowring A, Maumet C and Nichols TE (2018) Exploring the impact of analysis software on task fMRI results. *Hum Brain Mapp* 40(11): 3362–3384.
- Cammoun L, Gigandet X, Meskaldji D, et al. (2012) Mapping the human connectome at multiple scales with diffusion spectrum MRI. *Journal of Neuroscience Methods* 203(2): 386–397.
- Denis C, Castro PDO and Petit E (2016) Verificarlo: checking floating point accuracy through Monte Carlo Arithmetic. In: *2016 IEEE 23rd symposium on computer arithmetic (ARITH)*, pp. 55–62.
- Frechtling M and Leong PHW (2015) MCALIB: measuring sensitivity to rounding error with Monte Carlo programming. *ACM Transactions in Programming Language Systems* 37(2): 5:1–5:25.
- Garyfallidis E, Brett M, Amirbekian B, et al. (2014) Dipy, a library for the analysis of diffusion MRI data. *Frontiers in Neuroinformatics* 8: 8.
- Glatard T, Lewis LB, Ferreira da Silva R, et al. (2015) Reproducibility of neuroimaging analyses across operating systems. *Frontiers in Neuroinformatics* 9: 12.
- Jenkinson M, Beckmann CF, Behrens TEJ, et al. (2012) FSL. *Neuroimage* 62(2): 782–790.

- Kiar G (2019) BIDS app—FSL diffusion preprocessing (Version 5.0.9). Zenodo. DOI: 10.5281/zenodo.2566455.
- Kiar G, Brown ST, Glatard T, et al. (2019) A serverless tool for platform agnostic computational experiment management. *Frontiers in Neuroinformatics* 13: 12.
- Klein A, Andersson J, Ardekani BA, et al. (2009) Evaluation of 14 nonlinear deformation algorithms applied to human brain MRI registration. *Neuroimage* 46(3): 786–802.
- Kurtzer GM, Sochat V and Bauer MW (2017) Singularity: scientific containers for mobility of compute. *PLoS One* 12(5): e0177459.
- Lewis LB, Lepage CY, Khalili-Mahani N, et al. (2017) Robustness and reliability of cortical surface reconstruction in CIVET and FreeSurfer. In: *Annual Meeting of the Organization for Human Brain Mapping*. http://www.bic.mni.mcgill.ca/users/llewis/CIVET_vs_FS_HBM2017_final.pdf
- Nooner KB, Colcombe SJ, Tobe RH, et al. (2012) The NKI-Rockland sample: a model for accelerating the pace of discovery science in psychiatry. *Frontiers in Neuroscience* 6: 152.
- Parker DS (1997) *Monte Carlo Arithmetic: exploiting randomness in floating-point arithmetic*. Computer Science Department, University of California (Los Angeles).
- Peng RD (2011) Reproducible research in computational science. *Science* 334(6060): 1226–1227.
- Sawaya G, Bentley M, Briggs I, et al. (2017) FLiT: cross-platform floating-point result-consistency tester and workload. In: *2017 IEEE international symposium on workload characterization (IISWC)*, Seattle, WA, USA, 1–3 October 2017, pp. 229–238. IEEE.
- Skare S, Hedehus M, Moseley ME, et al. (2000) Condition number as a measure of noise performance of diffusion tensor data

acquisition schemes with MRI. *Journal of Magnetic Resonance* 147(2): 340–352.

Author biographies

Gregory Kiar is a PhD candidate in Biomedical Engineering at McGill University where he studies the stability of neuroimaging pipelines.

Pablo de Oliveira Castro is Computer Science Assistant Professor at the Université de Versailles St-Quentin-en-Yvelines.

Pierre Rioux is a software architect in the McGill Centre for Integrative Neuroscience.

Eric Petit is a research engineer and HPC application specialist at Intel Exascale Computing Research Lab.

Shawn T Brown is the Director of the Pittsburgh Super-Computing Center.

Alan C Evans is the Director of the McGill Centre for Integrative Neuroscience and James McGill Professor of Neurology and Neurosurgery at McGill University.

Tristan Glatard is a Computer Science and Computer Engineering Associate Professor at Concordia University.